# Supporting Information

## Ding et al. 10.1073/pnas.1320644111

### SI Materials and Methods

**Analysis of Supercoils Constrained by CI-Mediated Looping of Plasmids.** Before nicking a mixture (320 μL) containing 0.156 nM of negatively supercoiled DNA template and 170 nM or various concentrations of wild-type λ repressor (CI) in 20 mM Tris-acetate (pH 7.9 at 25 °C), 50 mM potassium acetate, 10 mM magnesium acetate, 1 mM DTT was assembled on ice and incubated for 30 min at 37 °C. Then, the supercoiled DNA templates were digested by 20 units of Nb.BbvCI at 37 °C for 15 s. Next, a large excess (289 nM) of a double-stranded oligonucleotides containing the Nb.BbvCI recognition site (top strand, 5′-CGGCATGGCGGCCCTATGCTGAGGACTCGGCCGACGCGCT-3′) was added to the reaction mixtures to inhibit further plasmid digestion. The nicked DNA templates were ligated using 800 units of T4 DNA ligase in the presence of 1 mM ATP at 37 °C for 5 min, and the reaction was terminated by extraction with an equal volume of phenol. Plasmids were precipitated in ethanol and dissolved in 25 μL of 10 mM Tris·HCl buffer (pH 8.5). The ligated DNA products were separated using 1% agarose gel electrophoresis in the absence or presence of 1 μg/mL chloroquine, and the superhelicity of topoisomers was calculated from the gel images stained with ethidium bromide using KODAK 1D Image Analysis Software. Experiments were repeated three times, and the results were averaged.

**Determining the Superhelical Density of Supercoiled Plasmids Before Addition of CI.** One hundred-microliter mixtures containing 1.5 μg of negatively supercoiled DNA template, 200 nM *Escherichia coli* DNA topoisomerase I, and various concentrations of ethidium bromide in 20 mM Tris-acetate (pH 7.9 at 25 °C), 50 mM potassium acetate, 10 mM magnesium acetate, 1 mM DTT, and 10 μg/mL BSA were assembled on ice and incubated for 15 min at 37 °C. The reactions were terminated by extraction with an equal volume of phenol. The DNA topoisomers were isolated and subjected to 1% agarose gel electrophoresis in the absence or presence of 0.5, 1, or 2.5 μg/mL of chloroquine for the determination of the supercoiling density (1).

**Preparation of DNA Tethers for Magnetic Tweezers.** DNA constructs for magnetic-tweezers experiments were formed by tether segments of either 4.4, 4.9, or 5.5 kbp containing the λ oL and oR regulatory regions ligated to biotin-labeled and digoxigenin-labeled attachment fragments at opposite ends using T4 DNA ligase [New England Biolabs (NEB)]. Tether segments with four different separations between the oL3 and oR3 sites (loop lengths) were produced (see Tables S1 and S2 and Dataset S1 for DNA constructs). Biotin- or digoxigenin-labeled end fragments of 800–1,000 bp were created using PCR (KOD Hot Start Polymerase kit; Novagen) with the appropriate primer pairs and templates (Tables S1 and S2) to incorporate about 5–10% (mol/mol) biotin- or digoxigenin-labeled dUTP. Double digestions were used to generate complementary ends for ligation to the central DNA fragments. All restriction enzymes were from NEB.

The DNA constructs were attached at one end to the anti-digoxigenin–coated glass surface of a flow chamber and at the other end to a 1.0-μm–diameter streptavidin-coated, paramagnetic bead (Dynabead MyOne Streptavidin T1; Invitrogen). Multiple biotin–streptavidin or digoxigenin–anti-digoxigenin bonds at bead and glass surfaces, respectively, torsionally constrained the tethers. Flow microchambers of ∼50-μL volume were assembled between two glass coverslips spaced by double-sided scotch tape and lined with silicon grease. Before experiments, DNA tethers were incubated for at least 1 h at either room temperature or 4 °C in λ buffer (10 mM Tris·HCl, pH 7.4, 0.1 mM EDTA, 200 mM KCl, 0.2 mM DTT, 5% DMSO, and 0.2 mg/mL α-casein).

**Manipulation of DNA Tethers with Magnetic Tweezers.** For single-molecule experiments, DNA was stretched and twisted using a pair of permanent magnets on a mount above the microscope stage, which could be both translated along and rotated about the optical axis of the microscope. First, torsionally constrained, single DNA tethers were identified by twisting. The tethers were unwound to $\sigma \sim -10\%$ (−42 turns for ∼4,950-bp DNA), rewound to +10%, unwound to −10% again, and unwound back to 0 in steps of three turns while recording the extension. These extension vs. twist curves were symmetric for both undertwisting and overtwisting at low tension, 0.2 pN, as plectonemes formed and reduced the extension. Instead under high tension, ∼3 pN, although plectonemes still formed with overtwisting, undertwisted DNA underwent a phase transition to denatured or left-handed helices and the maxima of such curves indicated the contour lengths of torsionally relaxed DNA (2). Multiply tethered beads that do not exhibit this phase change were discarded. Then, single tethers were gently stretched at low tension and twisted after the addition of CI protein diluted in λ buffer to a final concentration of 160 nM (393-bp loops) or 200 nM (all other loops). Wild-type CI protein from the laboratory of Sankar Adhya (NIH, Bethesda, MD) was used for experiments with 393-bp loops, and a His-tagged CI (3) provided by Keith Shearwin (University of Adelaide, Adelaide, SA, Australia) was used with all other loops. Wild-type and His-tagged CI proteins behave identically in looping experiments in vitro (4). Two types of experiments were performed. In one, the tether extension as a function of mechanically introduced twist, was recorded at constant tensions between 0.1 and ∼0.8 pN without protein present. Then it was repeated with CI to detect the superhelical density ($\sigma_L$) constrained in λ repressor-mediated loops that formed spontaneously in extensively twisted DNA. The value of $\sigma_L$ was equal to the shift (units of turns) of the reduced extension vs. twist curve divided by the number of helical turns in a relaxed DNA segment of the length of the loop, $Lk_0$. In another experiment, extension was recorded with or without CI protein as a function of time under constant tensions and levels of $\sigma$ to monitor spontaneous loop formation and breakdown. In this case, useful values of $\sigma$ were limited to a range without extensive plectoneme formation in which unlooped and looped states were distinct.

**Analysis of Magnetic Tweezer Data.** Using video-rate, 3D tracking, *X*, *Y*, and *Z* coordinates of mobile (tethered) and nonspecifically stuck beads were acquired at 10 frames per s. From the extension of the tether along the microscope axis and the transverse excursions of the tethered bead perpendicular to the direction of the magnetic field, the tension in the molecule was determined using the equipartition theorem. The time vs. extension data were then analyzed to identify probable looping events. A Matlab-coded "change-point" algorithm and expectation-maximization routine (5, 6) was used to parse the time series for looped and unlooped states without filtering or averaging which limit the time resolution. The looped ($\tau_L$) and unlooped ($\tau_U$) lifetimes and the associated uncertainties were determined by optimization of the maximum-likelihood function for an exponential distribution with at least 150 data points. The energy associated with looping under various tension and twist conditions

was calculated using $\Delta G/kT = -\ln(\tau_L/\tau_U)$. Error bars were 99% confidence intervals for mean lifetimes determined from the exponential fit or the propagation of errors from lifetime measurements in the calculation of looping energies.


1. Clark DJ, Leblanc B (2009) Analysis of DNA supercoiling induced by DNA-protein interactions. *Methods Mol Biol* 543:523–535.
2. Sarkar A, Léger JF, Chatenay D, Marko JF (2001) Structural transitions in DNA driven by external force and torque. *Phys Rev E Stat Nonlin Soft Matter Phys* 63(5 Pt 1):051903.
3. Nickels BE, Dove SL, Murakami KS, Darst SA, Hochschild A (2002) Protein-protein and protein-DNA interactions of σ70 region 4 involved in transcription activation by lambdacI. *J Mol Biol* 324(1):17–34.
4. Gao N, Shearwin K, Mack J, Finzi L, Dunlap D (2013) Purification of bacteriophage lambda repressor. *Protein Expr Purif* 91(1):30–36.
5. Manzo C, Finzi L (2010) Quantitative analysis of DNA-looping kinetics from tethered particle motion experiments. *Methods In Enzymology*, ed Nils GW (Academic, San Diego), Vol 475, pp 199–220.
6. Watkins LP, Yang H (2005) Detection of intensity change points in time-resolved single-molecule measurements. *J Phys Chem B* 109(1):617–628.


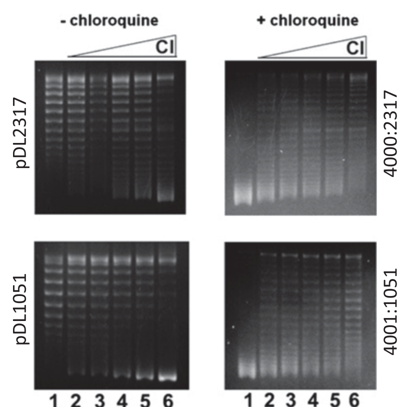


**Fig. S1.** λ repressor (CI) divided supercoiled plasmids into two independent topological domains. The DNA-nicking assays were performed as described in *Materials and Methods*. In addition to 0.156 nM of either plasmid pDL1051 or pDL2317 with intact:nicked segments of 4,001:1,051 or 4,000:2,317 bp, the reaction mixtures also contained 0, 10, 20, 52, 80, or 170 nM λ cI (lanes 1–6, respectively) and Nb.BbvCI (20 units). The DNA molecules (topoisomers) were isolated and subjected to agarose gel electrophoresis in absence (–) or presence (+) of 2.5 μg/mL chloroquine. Leftmost lanes (1) contains DNA relaxed at 37 °C and slightly (+) supercoiled because the gels were run at 24 °C.

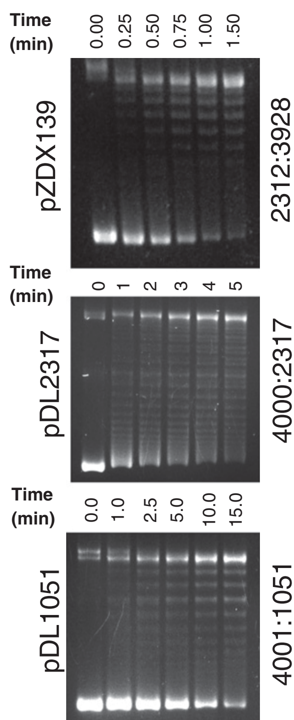


**Fig. S2.** DNA-nicking assays in the presence of 170 nM CI were performed as described in *Materials and Methods* with incubation at 37 °C. At the indicated times, the DNA was isolated and topoisomers were separated using agarose gel electrophoresis without chloroquine.

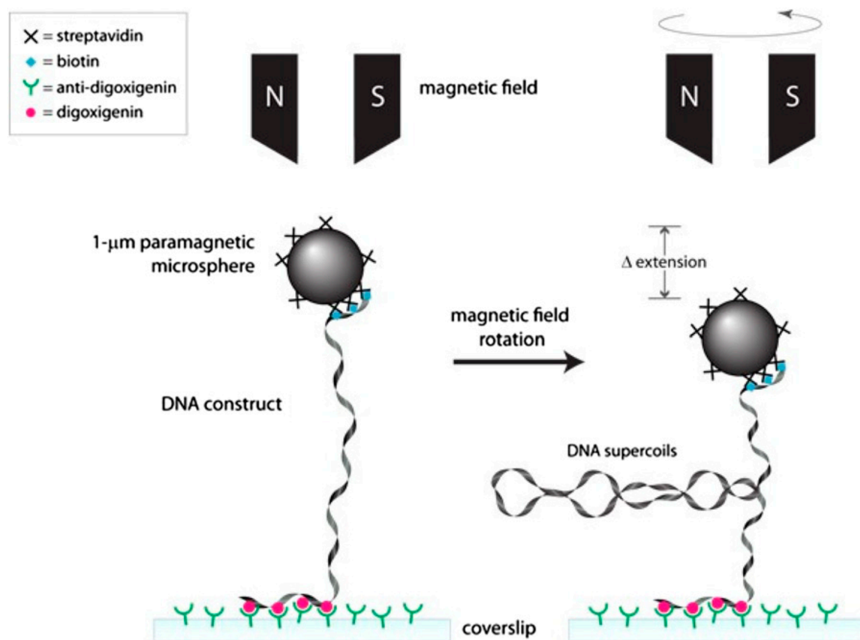


**Fig. S3.** Schematic diagram of a magnetic tweezer apparatus used to twist and stretch DNA (not to scale). A streptavidin-labeled, paramagnetic microsphere is tethered to an anti-digoxigenin–coated glass surface using DNA labeled at opposite ends with biotin and digoxigenin. Permanent dipole magnets brought to within a few millimeters induce a dipole in the microsphere to attract and rotationally orient it. This generates slight tension in the DNA tether, which can be modulated by changing the separation between the magnets and the bead. Turning the magnets turns the rotationally coupled microsphere and twists the DNA which eventually can form plectonemes (supercoils). Monica Fernandez (Department of Physics, Emory University, Atlanta) kindly allowed us to use the illustration in Fig. S3.

PNAS PNAS PNAS PNAS

**Fig. S4.** A gallery of extension vs. twist curves in which CI-secured loops trapped various levels of superhelical density. Traces represent data acquired as the tether was twisted without protein (black) or with protein from (+) to (–) (blue) or (–) to (+) (red). The lower abscissa encodes the overall linking number of the unlooped tether. The upper abscissa encodes the value of superhelical density trapped in CI-mediated looped molecules on the basis of the observed shifts.

**Fig. S5.** The trapping of superhelical density by plectoneme-catalyzed CI-mediated loops and subsequent rupture. Levels of superhelical density constrained in 2,317- or 1,051-bp DNA loops observed in experiments as shown in Fig. 2 ranged from −15% to +11% under tensions of 0.2–0.4 pN. Note that, although the tethers were mechanically twisted to introduce only between ±10% superhelical density, the looped segment trapped 11% several times and 15% once.

Fig. S6. Formation and rupture of 393-bp loops mediated by CI in DNA with $\sigma = -1.4\%$ under 0.5 pN of tension. (*A*) Representative recordings of tether extension vs. time (*Left*) exhibited transitions in the presence of 160 nM CI (black) but not in the absence of CI (gray). Peaks in a histogram (*Right*) for this single DNA tether identify looped and unlooped states. When the superhelical density of DNA was positive, loops were rare and short-lived. In fact, with about +1% superhelical density and 0.2 pN of tension, only four events, lasting about 2 s each, were observed during hours of recording. Furthermore, loops never formed in rotationally relaxed DNA. Instead, looping occurred in negatively supercoiled DNA at tension less than or equal to 0.8 pN. (*B*) Intervals of looped (red) and unlooped (black) lifetimes for the entire set of recordings in the presence of 160 nM CI were fitted with single-exponential decays to determine mean lifetimes.

Fig. S7. An example calculation of the mean lifetime for unlooped (black) and looped (red) states for a DNA tether with CI operator sites separated by 1,051 bp under 0.4-pN tension and unwound by $-1.8\%$ $\sigma$ (−8.5 turns). The lifetimes of looped and unlooped states were determined using the change-point algorithm, binned and plotted as histograms, and fitted with single-exponential decay functions.

**Fig. S8.** For DNA tethers under different applied tensions and supercoiling levels for different loop sizes, the calculated mean lifetimes of unlooped (black) and looped (red) states varied from 2 to 35 s. For 393-bp loops, unlooped lifetime (black) decreased and looped lifetime (red) increased as the supercoiling density became more negative. For 1,051-bp loops, the mean lifetime of the unlooped state still decreased as negative supercoiling increased, but the mean lifetime of the looped state fluctuated around 5 s. For even larger loops of 1,231 or 1,662 bp, mean lifetimes fluctuated with no clear trends.

**Table S1. DNA constructs**

| DNA amplicon or main tether name | Length, bp | Labeled nucleotide | Template | | Primers | | Restriction site | Template reference |
|---|---|---|---|---|---|---|---|---|
| | | | Name | Length, bp | Forward | Reverse | | |
| 393-biotail | 732 | bio-dUTP | λ | 48,502 | λbiotailF | λbiotailR | NheI | GenBank accession no. J02459.1 |
| 393-digtail | 1,172 | dig-dUTP | λ | 48,502 | λdigtailF | λdigtailR | NarI | GenBank accession no. J02459.1 |
| 393-main | 4,379 | — | pDL944 | 4,396 | NAR | NHE | NarI and NheI | Ref. 1 |
| 1,051-biotail | 921 | bio-dUTP | pDL1051 | 5,052 | S/pDL2317/2526 | A/pDL2317/3645 | DraIII-HF | Ref. 2 |
| 1,051-digtail | 929 | dig-dUTP | | | S/pUC19/2019 | A/208–12/337 | NgOMIV | |
| 1,051-main | 4,948 | — | | | — | — | NgOMIV and DraIII-HF | |
| 1,231-biotail | 820 | bio-dUTP | pDL955 | 5,252 | S/pDL2317/2526 | A/pDL2317/3645 | NgOMIV | Courtesy of D. Lewis (S. Adhya Laboratory, NIH; unpublished) |
| 1,231-digtail | 1,221 | dig-dUTP | | | S/pUC19/2019 | dig-control | HindIII | |
| 1,231-main | 4,959 | — | | | — | — | HindIII and NgOMIV | |
| 1,662-biotail | 797 | bio-dUTP | pDL950 | 5,683 | S/pDL2317/2526 | A/pDL2317/3645 | NcoI | Courtesy of D. Lewis (S. Adhya Laboratory, NIH; unpublished) |
| 1,662-digtail | 923 | dig-dUTP | | | S/pDL2317/2526 | A/pDL2317/3645 | DraIII-HF | |
| 1,662-main | 4,983 | — | | | — | — | NcoI and DraIII-HF | |
| 2,317-biotail | 901 | bio-dUTP | pDL2317 | 6,318 | S/pDL2317/2526 | A/pDL2317/3645 | BamHI | Ref. 3 |
| 2,317-digtail | 921 | dig-dUTP | | | S/pDL2317/2526 | A/pDL2317/3645 | DraIII-HF | |
| 2,317-main | 5,515 | — | | | — | — | BamHI and DraIII-HF | |

Main fragments for DNA tethers for magnetic tweezers experiments were constructed using digestion of plasmids and PCR templates listed above. Restriction enzymes were then used to generate "sticky" ends for ligation to PCR-generated biotin- or digoxigenin-labeled attachment fragments (biotail or digtail). The primer sequences are given in Table S2.

1. Lewis D, Le P, Zurla C, Finzi L, Adhya S (2011) Multilevel autoregulation of λ repressor protein CI by DNA looping in vitro. *Proc Natl Acad Sci USA* 108(36):14807–14812.
2. Zurla C, et al. (2006) Novel tethered particle motion analysis of CI protein-mediated DNA looping in the regulation of bacteriophage Lambda. *J Phys Condens Matter* 18(14):S225–S234.
3. Zurla C, et al. (2009) Direct demonstration and quantification of long-range DNA looping by the λ bacteriophage repressor. *Nucleic Acids Res* 37(9):2789–2795.

**Table S2. Primer sequences**

| Primer name | DNA sequence, 5′ to 3′ |
|---|---|
| NAR | TCCAGAGGCGCCCTCACCGGCTCCAGATTTATCAGCAATAAACCAGCCAGCCGGAAGGGCCGAGCGC |
| NHE | TGGTAAGCTAGCCTGGGGCCAGATGGTAAGCCCTCCCGTATCGTAGTTATCTACACGACGGGGAGTCAGG |
| λbiotailR | TAAGCAGAAGGCCATCCTG |
| λbiotailF | CTGCCTCTTTCTCTTCACGG |
| λdigtailR | CTGGCCCTGCTTATTACAGGATGTGCTCAACAGACGTTTACTGTTCAAAACAAACCG |
| λdigtailF | CTGATAACGGACGTCAGAAAACCAGAAATCATGGTTATGACGTCATTGTAGGCGGAGAGC |
| S/pDL2317/2526 | TGTATGGAACAACGCATAAC |
| S/pDL2317/3645 | TCCAAACTGGAACAACAC |
| A/208–12/337 | TGGCGTAATAGCGAAGAG |
| S/pUC19/2019 | TGCACAACATGGGGGATCAT |
| dig-control | GACTGATAGTGACCTGTTCGTTGCAACAAATTGATAAGCAATGC |
| S/pUC19/2412 | TGGGTGAGCAAAAACAGGAAGGCA |
| A/pUC19/1435 | CGTAATCTGCTGCTTGCAA |

# Other Supporting Information Files

Dataset S1 (PDF)